PHYSICAL REVIEW E, VOLUME 64, 011708

Liquid-crystal–electrochromic-material interface: A *p*-*n*-like electro-optic junction

Anca-Luiza Alexe-Ionescu,[1] Andrei Th. Ionescu,[2] Nicola Scaramuzza,[3,*] Giuseppe Strangi,[3] Carlo Versace,[3]
Giovanni Barbero,[4] and Roberto Bartolino[3]

[1]*Departamentul de Matematica si Fizica, Universitatea Politehnica din Bucuresti, Splaiul Independentei 313,*
Ro-77206 Bucharest, Romania

[2]*Facultatea de Fizica, Universitatea din Bucuresti, P.O. Box MG-11, Ro-76900 Bucharest, Romania*

[3]*Dipartimento di Fisica dell'Universita della Calabria and Istituto Nazionale per la Fisica della Materia,*
I-87036 Arcavacata di Rende (Cosenza), Italy

[4]*Dipartimento di Fisica del Politecnico di Torino and Istituto Nazionale per la Fisica della Materia, Corso Duca degli Abruzzi 24,*
I-10129 Torino, Italy

(Received 3 October 2000; revised manuscript received 9 February 2001; published 27 June 2001)

A liquid crystal (LC) cell has been made by using a standard sandwich configuration with one of the indium tin oxide (ITO) electrodes covered by a thin layer of tungsten trioxide (WO_3). In this kind of cell optical polarization switching (observed under a crossed polarizer microscope) occurs for only one of the two polarities of an ac external applied electric field, while in the usual liquid crystal cells the electro-optic response does not depend on the sign of the field. The inhibiting switching configuration corresponds to anodic polarization of the tungsten trioxide film in which the deintercalation of cations occurs. Here we present the time behavior of charge and discharge for both the anodic and cathodic currents. A model based on charge carrier exchange between the ITO-WO_3 and WO_3-LC interfaces and also electrochemical processes is reported. Our model is also capable of explaining the electric and electro-optic asymmetric responses of the cell. Numerical calculations confirm the model.

DOI: 10.1103/PhysRevE.64.011708 PACS number(s): 61.30.−v

I. INTRODUCTION

Nematic liquid crystals (NLC's) have been much used in many devices like displays, spatial light modulators, light valves, etc. Because the NLC internal order is very sensitive to both external fields and the properties of boundary surfaces, they can be used to modulate light by electro-optic response. An applied electric field can alter the order of a NLC induced by the surfaces. In fact, the nematic director **n** is changed by the dielectric torque, which is proportional to the dielectric anisotropy $\epsilon_a = \epsilon_\parallel - \epsilon_\perp$ ($\epsilon_\parallel$ and $\epsilon_\perp$ being the dielectric permittivities parallel and perpendicular to the optical axes, respectively). This electrically controlled birefringence results in variation of the transmitted light between crossed polarizers (optical switching).

It is known that in the usual nematic cells the electro-optic response does not depend on the sign of the applied electric field. In asymmetric cells, however, optical switching can be seen for only one direction of the applied field. For instance, such an asymmetric cell has been prepared by mixing with the nematic liquid crystal a small amount of UV polarizable monomer. On irradiating the cell from one face, a polymer network of decreasing density appears within the liquid crystal, which also produces a gradient of fixed charges. This gradient, in turn, causes a nonsymmetric injection of current into the cell [1].

Another way of getting asymmetric cells is to insert a thin layer of amorphous tungsten trioxide (WO_3) onto a conductive indium tin oxide (ITO) deposited glass [2–4]. Recently, we have also observed a polarity dependent electro-optic response in asymmetric cells in which, instead of the amorphous tungsten trioxide layer, a proton doped thin layer of polymer has been coated on one of the glass plates that make up the planar capillary cell [5].

In this paper we focus our analysis on nematic liquid crystal cells with a WO_3 layer. Tungsten trioxide is an amorphous material that presents a large inner surface favoring ionic exchange during chemical reactions. It also has electrochromic properties, i.e., it may change its color depending on the quantity of positive ions (protons) it can adsorb. The phenomenon of color change was explained some years ago as a simultaneous injection of free electrons and hydrogen cations H^+ during the formation of tungsten bronze [6–8]. In the presence of an external electric field the process of intercalation and deintercalation of positive ions (protons) into the WO_3 layer can cause an asymmetric space charge, voltage drop, and current injection in asymmetric liquid crystal cells.

As shown in Fig. 1 (see also Fig. 1 of Ref. [4]), a NLC cell is made as a planar capillary using two support glasses. Each of the two glasses has deposited on one face a very thin

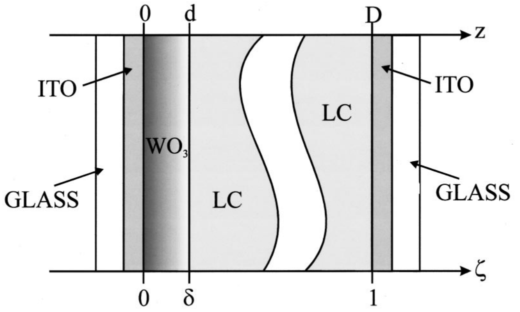

FIG. 1. A schematic drawing (not to scale) of the cell used in experiments.

---

[*] Author to whom correspondence should be addressed.

1063-651X/2001/64(1)/011708(10)/$20.00

©2001 The American Physical Society

layer of indium tin oxide, which behave like high resistance conductive layers (20 Ω/□) and form the interior boundaries of the cell. A layer of tungsten trioxide was deposited by radio frequency sputtering on top of the ITO layer of only one of the glass plates. The tungsten trioxide layer is amorphous and extremely porous [2,3,4,6–8].

The sample plates were fixed at a distance of 8 μm apart by using Mylar spacers. The cell also constitutes an electric capacitor because on the two ITO surfaces two Ohmic contacts (made of indium-tin alloy) were soldered. The cell was filled with a nematic liquid crystal known commercially as BL001 by Merck (formerly E7); it is a eutectic mixture of four different cyanobiphenyl compounds. The temperature range of the nematic mesophase is between 20 and 61 °C. The dielectric anisotropy (at 20 °C) is $\epsilon_a = \epsilon_\parallel - \epsilon_\perp = +13.8$. The filling of the space enclosed between the asymmetric glass plates with liquid crystal was done slowly enough to prevent any orientational alignment induced by the flow. Actually, as already reported [2–4], the tungsten trioxide layer induces a homogeneously planar alignment of the liquid crystal molecules (**n** parallel to the boundary surfaces) along a certain axis that depends on the process of sputtering. This direction was chosen to be perpendicular to the direction of filling the cell with the liquid crystal. The starting orientation of the NLC cell was set in such a way as to have a maximum of transmitted light when the cell was placed on the stage of a microscope [Axioskop Pol (Zeiss)] between crossed polarizers. When a dc (or very low frequency) voltage, above a certain threshold, is applied to our asymmetric NLC cell a transition from planar to homeotropic alignment is expected. This indeed happens, but only in the case of cathodic (negative) polarization (from now on we will consider the polarization with respect to the WO_3 side of the cell), when the transmitted light goes essentially to zero. In the case of anodic (positive) polarization, although for a very short time one can see a blackening of the optical field, a decrease of the electric field in the bulk below the threshold, possibly associated with some diffusion and turbulence, forces the image to become bright again.

The idea is that only in the case of anodic polarization are there transient currents injected into the cell which build up a sufficiently large surface charge. This surface charge—at the interfaces between the liquid crystal and the glass plates—produces an internal electric counterfield, which will inhibit the switching to the homeotropic state (Fig. 2). The building up of the surface charges is asymmetric, i.e., it depends on the sign of the applied field due to the changing of the proton concentration within the WO_3 layer.

In Ref. [4] electrical measurements (current, complex impedance, cyclic voltammetry) carried out on cells with WO_3 layers pointed out the role of the diffusion of protons and, as a consequence, that of the internal counterfield associated with that diffusion. Yet the asymmetric behavior is given by a complex of synergic phenomena, including electrochemical, transport, and equilibrium statistical processes. A good understanding of this effect, apart from possible technical applications, would be beneficial to a wider spectrum of researchers from electrochemists and material scientists to liquid crystal device designers.

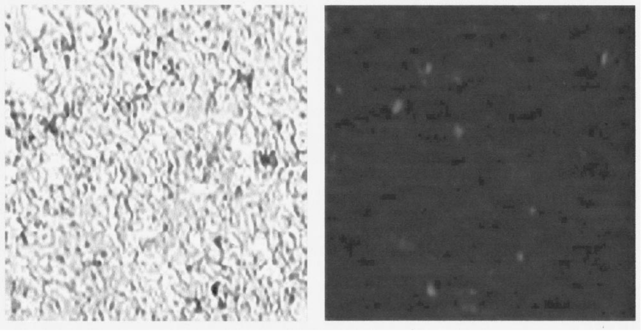

FIG. 2. Light transmitted through the cell with anodic (light) and cathodic (dark) polarizations.

In the following we want to explain why the free proton concentration has such an asymmetric impact on the sample. In Sec. II we present some experiments performed in order to have a better understanding of the phenomenon. In Sec. III we present a theory suited for explaining the asymmetric behavior of the electro-optic effect. Section IV concludes the paper.

II. EXPERIMENT

In order to understand better why these phenomena happen we have analyzed the electric properties of the cells. Already [2–4], the impedance behavior has shown a linear tail at small frequencies indicating a rather high conductivity. Using a sequence of positive, zero, and negative voltage pulses for 110 s each (Fig. 3), 200 current measurements were done for each voltage pulse—the time interval between successive current measurements being thus 0.55 s. In Fig. 4 we have plotted the time dependence of the current for the sequence +4, 0, −4, 0 V, and the plots reveal the following facts: (i) the time dependence of the currents is typical for charging or discharging capacitors; (ii) the anodic charging current is greater than the cathodic charging current; (iii) the discharge current following the anodic polarization is larger (in absolute value) than the discharge current that follows the cathodic polarization; (iv) an Ohmic current is also quite visible in the case of the anodic polarization; and (v) the time dependence of the anodic charging current is not a simple exponential function.

By integrating the currents one gets the charges that are stored in the cell. In order to minimize the influence of the

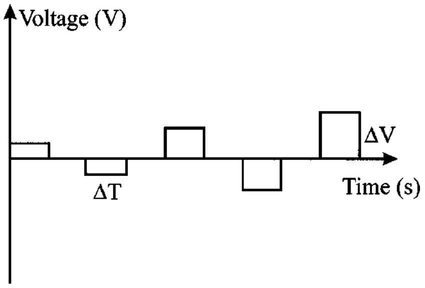

FIG. 3. Constant voltages applied to the cell when measuring the charging and discharging currents. $\Delta T = 110$ s.

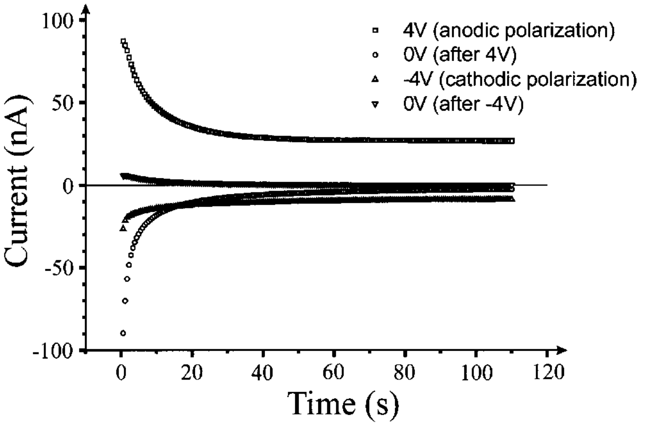

FIG. 4. Charging and discharging currents for the sequence 4, 0, −4, 0 V.

Ohmic currents when doing the integration we considered as the base that line which corresponds to the value of the current at the latest time instant. In Fig. 5 the stored charge densities are plotted versus the amplitudes (ΔV) of the voltage steps.

These results are even more interesting if we compare them to similar measurements made with a cell filled with the same nematogen liquid crystal E7 (Merck BL001) but with symmetric ITO deposited glass plates. In this case there is, of course, a complete symmetry of the current with respect to the polarity of the voltage steps but the charges stored in the cell are about three times smaller than in the case of the cell with insertion of a WO_3 film.

Then we wanted to see what would happen when instead of E7 liquid crystal we inserted a nonpolar organic oil *cis,trans*-decahydronaphthalene ($C_{10}H_{18}$) (DHN for short). In this case the charging and discharging currents are orders of magnitude smaller than in the case of E7-filled cells. The now poorer signal to noise ratio prevents one from distinguishing between the anodic and cathodic polarizations. In the case of DHN the estimated dielectric constant is ≈2 which is consistent with the value 2.1733 obtained by squaring the refractive index $n=1.4742$.

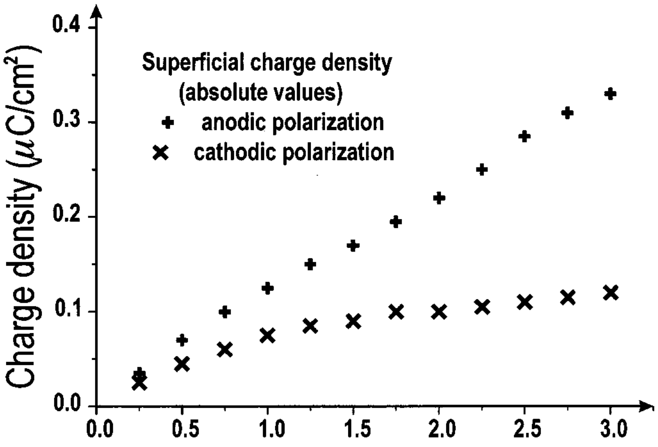

FIG. 5. Accumulated charge densities (absolute values) versus applied voltages in the two different polarizations.

As far as the LC E7 between ITO plates is concerned, the estimated stored charge density is ≈0.11 μC/cm^2 and in the case of cells with WO_3 its value is ≈0.12 μC/cm^2 for cathodic polarization and ≈0.36 μC/cm^2 for anodic polarization, which is equivalent to a dielectric constant in the range 10^3. Such a tremendous difference between E7 and DHN cannot be explained only by the fact that E7 (a mixture of cyanobiphenyls) is polar, but mainly by the fact that within E7 there are dissolved positive and negative ions. Even more, if in a cell with a WO_3 layer at cathodic polarization the charge density is slightly larger than in the case of a symmetric ITO/E7/ITO cell, when applying an anodic polarization the overall charge density triples. The fact that the stored charge density is so different for the two polarizations indicates that a process of charge compensation takes place in the layer of WO_3 during the cathodic polarization on one hand, and a liberation of new charge (protons) takes place during the anodic polarization on the other hand. We will use these facts in the following model.

As we have stressed from the beginning, WO_3 is a highly porous material. Inside its channels and voids there are sites that favor the reaction $H_2O \rightleftarrows H^+ + OH^-$, most probably because there are nonsaturated W bonds which can attract the oxygen of OH^-. A certain concentration of H^+ appears which eventually prevents the reaction going from left to right [9].

Note that WO_3 is also an electrochromic material. It can accept a large amount of cations (H^+, Li^+, Na^+, K^+) from a source to form nonstoichiometric tungsten bronze M_xWO_{3-y} according to

$$xM^+ + xe^- + WO_3 \rightleftarrows M_xWO_{3-y}, \qquad (1)$$

where M^+ are the cations and $0 \leqslant x \leqslant 0.5$ and $0 \leqslant y \leqslant 0.03$ [6]. When the value of x is large ($x > 0.1$) the tungsten bronze changes its color to blue. In our case the WO_3 film remains always transparent indicating that it is a dilute bronze. Also the fact that the stored charge density was between 300 and 900 nC/cm^2 μm for the trioxide tungsten film compared to the maximum observed stored charge density of 100 μC/cm^2 μm in WO_3 [10] tells us that we have a dilute bronze.

Let us first analyze the ITO-WO_3 interface alone. ITO has free electrons. They can diffuse into WO_3 pores where they force hydrogen to be bound by WO_3, forming regions of H_xWO_3 bronze. Figure 6 shows a scheme of this process. The ITO side of the interface remains positively charged whereas the WO_3 side of it remains with an unbalanced negative (localized OH^-) charge. The total (and local) concentration of H^+ has diminished so the reaction $H_2O \rightleftarrows H^+ + OH^-$ can proceed until the electric field from ITO toward WO_3 can now block the diffusion of electrons. A contact potential sets in. Connecting the two faces electrically, a current will flow, delivering electrons to the ITO side of WO_3, until all the water and/or the catalyst sites are used. The system works like an electric battery.

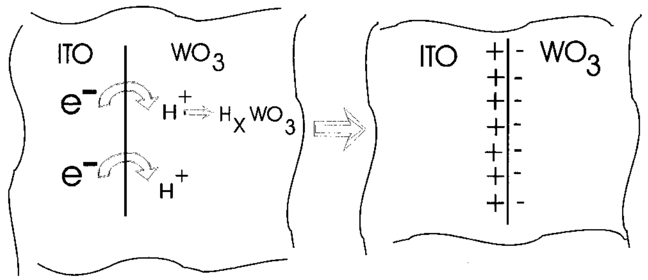

FIG. 6. A schematic drawing illustrating the process of hydrogen bronze formation expressed in Eq. (1).

If the ITO side is charged positively the protons in WO_3 are pushed to the right leaving an increased negative charge to the left. In the meantime a lack of protons on the left side of WO_3 causes Eq. (1) to go from left to right, creating an increased number of protons, which are pushed to the right. Hence, the total positive charge on the right side of the WO_3 layer becomes larger. If we consider n the concentration of negative (fixed) charges which does not vary and $n(z)$ the concentration of positive ions, there is a net negative charge q where $n(z)<n$, and there is an equal positive charge of the same magnitude where $n(z)>n$. A plot of positive and negative carrier concentrations across the WO_3 layer is shown in Fig. 7.

If now the ITO side is negatively charged, the protons are pulled to the left where they combine with a flux of ITO electrons. The stored charges are reversed but the new value q' is less than q due to hydrogen bronze formation (see Fig. 8). These two mechanisms, intercalation and deintercalation of protons at the left side of the WO_3 film, of which the latter seems to be more important, can explain quite easily why the discharge current following anodic polarization was larger than the discharge current that followed the cathodic polarization, i.e., the stored charges are different.

Now we have to take into account the role played by the liquid crystal. If the liquid crystal were a perfect dielectric, when applying an electric voltage across the cell the potential would vary linearly with distance and the electric field would be constant. In contrast, if the liquid crystal contains a certain amount of free ions, there will be a buildup of negative charge on the anodic side of the cell and a similar buildup of positive charge on the other side. The electric potential will no longer have a linear dependence and the electric field will not be constant. It will present a lower value in the bulk of the liquid crystal layer and higher values close to the surfaces. Figure 9 shows the two cases mentioned above. The larger the boundary charges, the higher are the values of the field near the surface and the lower is the field in the bulk. (One must not forget that the total area under the field plot is equal to the voltage across the liquid crystal.) These two boundary charges tend to screen the charges on the WO_3–liquid-crystal or liquid-crystal–ITO interfaces. Considered alone they are the sources of an internal field whose estimation was performed experimentally and presented in detail in [4].

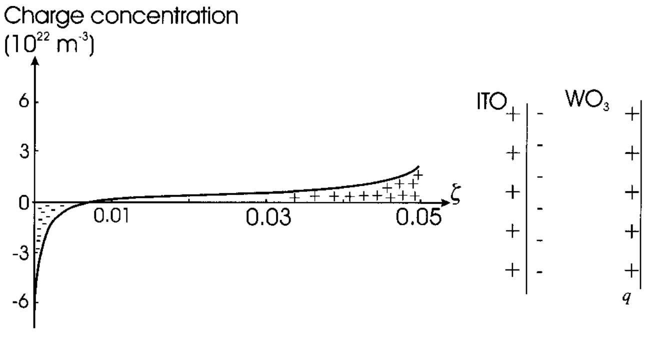

FIG. 7. Charge concentration of protons in WO_3 with anodic polarization.

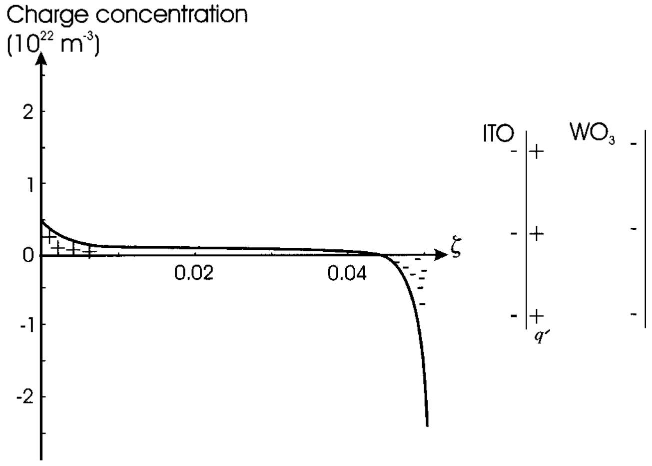

FIG. 8. Charge concentration of protons in WO_3 with cathodic polarization. The absolute values are about three times smaller than in Fig. 7.

If the cell is not symmetric, i.e., it has one thin layer of WO_3, when anodically polarized the positive charge q in WO_3 close to the interface with the liquid crystal will attract a large quantity of negative free ions within the liquid crystal. The same amount of positive charge will be on the ITO side of the liquid crystal. When the cell is cathodically polarized the charge q' is smaller than q and the corresponding buildup charges in the liquid crystal are smaller. The important result is that for a convenient voltage range the electric

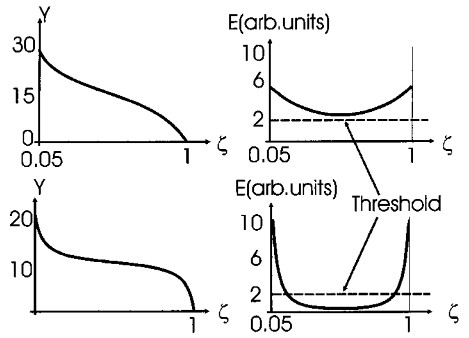

FIG. 9. The trend of the electric potential in liquid crystal region (left) and the electric field (right) for the two cases of polarization, anodic (down) and cathodic (up). For a better comparison the algebraic sign was disregarded.

field in the bulk of the liquid crystal will be lower in the case of anodic polarization than in the case of cathodic polarization in such a way as to be below the transition threshold for anodic polarization but above the threshold for cathodic polarization (see Fig. 9 again). Even the strong electric field that appears within a layer of around the Debye length [11] cannot align the liquid crystal molecules homeotropically because of the rather strong planar anchoring. Also, there the injected currents are not negligible. In fact the asymmetry of the injected currents is due to the rectifying properties of the ITO/WO_3 junction, which induces on the interface between WO_3 and the liquid crystal a depletion layer of free charges when the cell is cathodically polarized with respect to the WO_3 face. In the case of anodic polarization there is also an increase of the positive mobile carriers in a layer of around the Debye length at the WO_3–nematic-LC interface which injects a current having the same sign as that injected by ITO at the other face. Both currents having the same direction create a rather strong current which inhibits the homogenous alignment. Without the WO_3 layer, for each polarization, electrons can be injected on one ITO side whereas on the other ITO interface there is no injection. So the current is alternately blocked on one or the other of the two interfaces. If we consider that the cell has two switches, these work in counterphase when the cell is symmetric but the WO_3 layer reverses the phase of one switch so now they are in phase: on or off. Very recent measurements have shown that the same effect can be obtained with a thin layer of nickel hydroxide doped with Li^+ ions. The same process of creating a pair of depleted or enhanced layers of positive mobile ions is responsible for this effect.

One important task is to see which process is more important: the lowering of the electric field below the threshold or the symmetry of the injected currents? To answer this question, at least qualitatively, we tried to see if a large capacitor inserted in series with the cell would modify the asymmetry of the electro-optic effect. The result was negative, i.e., the asymmetry still exists although the frequency limit for this asymmetry was lowered a little. The capacitor was chosen with such a value as to have the same voltage drop across the sample as in the case without the capacitor. The buildup of surface charges is the same, but now the injected currents are essentially blocked. Of course, the much higher time constant of the system lowers the frequency limit. This experiment suggests that in this case, although one cannot completely rule out the influence of the injected currents, the lowering of the electric field in the bulk of the liquid crystal when the sample is anodically polarized plays the most important role.

III. THEORY

The chemical potential of the positive ions may be written as

$$\mu = eV(z) + kT \ln n(z), \tag{2}$$

where $n(z)$ is the concentration of positive ions and $V(z)$ is the electric potential experienced by the protons inside WO_3. From the equilibrium requirement that the chemical potential be uniform throughout the distribution of positive ions, we get

$$n(z) = n(\overline{z}) \exp\left(- \frac{e[V(z) - V(\overline{z})]}{kT} \right) = n(\overline{z}) \exp[-\Psi(z)], \tag{3}$$

where, for $z \in [0,d]$, we use an adimensional potential $\Psi_1(z) = eV(z)/kT$. Let $\Psi_1(0) = \Psi_0$, the potential of the ITO/WO_3 interface. We speak of the anodic case if $\Psi_0 > 0$ and of the cathodic case if $\Psi_0 < 0$. The other contact (liquid-crystal–ITO interface) is grounded. Consequently,

$$\Psi_1(\overline{z}) = \frac{eV(\overline{z})}{kT} \quad \text{and} \quad \Psi(z) = \Psi_1(z) - \Psi_1(\overline{z}), \quad \Psi(\overline{z}) = 0. \tag{4}$$

If n is the constant concentration of negative charges (OH^-), we shall choose $\overline{z}$ as the root of the equation $n(z) = n$, i.e., the surface within the WO_3 layer where the net charge density is zero. Considering that the entire layer of WO_3 does not have any net charge, the following condition has to be fulfilled:

$$nd = \int_0^d n(z)dz = n(\overline{z}) \int_0^d \exp[-\Psi(z)]dz,$$

or

$$\frac{1}{d} \int_0^d \exp[-\Psi(z)]dz = 1. \tag{5}$$

One further important fundamental equation will be required. This is the well known Poisson equation

$$-\epsilon_0 \epsilon_1 \frac{d^2V(z)}{dz^2} = e[n(z) - n] \tag{6}$$

or

$$\frac{d^2\Psi(z)}{dz^2} = - \frac{e^2 n}{\epsilon_0 \epsilon_1 kT} \{\exp[-\Psi(z)] - 1\}. \tag{7}$$

It is convenient to use a new adimensional coordinate

$$\zeta = \frac{z}{D}, \tag{8}$$

where D is the total thickness of the cell (including the thickness d of the WO_3 layer). Let

$$\delta = \frac{d}{D}, \quad L_1^2 = \frac{\epsilon_0 \epsilon_1 kT}{2ne^2}. \tag{9}$$

Equation (7) becomes

$$\frac{d^2\Psi(\zeta)}{d\zeta^2} = - \frac{D^2}{2L_1^2} \{\exp[-\Psi(\zeta)] - 1\}, \tag{10}$$

where $L_1=\sqrt{\epsilon_0\epsilon_1 kT/2ne^2}$ is the so called Debye screening length, ϵ_1 is the dielectric constant of WO_3, and $e=+1.6\times10^{-19}$ C. The dielectric constant ϵ_1 is typically about 6; it may depend on the porosity of the WO_3 layer or whether the tungsten trioxide has been annealed or not. This value has nothing to do with our previous assertion that the equivalent dielectric constant of the cell was of the order of 10^3. That was due entirely to the mobile charges dissolved within the liquid crystal and to the protons in WO_3. In other words, ϵ_1 is the dielectric constant of a pure matrix of tungsten trioxide free of charges. Experimentally, it may be measured in an ac field having a frequency much lower than the IR (or optical) absorption, but higher than the reciprocal of the diffusion time of (almost) free protons. One must also take into account that the average concentration of free protons is $\approx 10^{-6}$ that of WO_3 molecules, so the protons may be considered as independent charges in a dielectric matrix. The same argument will be considered when the liquid crystal is concerned.

Condition (5) becomes

$$\frac{1}{\delta}\int_0^{\delta}\exp[-\Psi(\zeta)]d\zeta=1. \tag{11}$$

It can be easily proved that Eq. (10) is equivalent to

$$\left(\frac{d\Psi(\zeta)}{d\zeta}\right)^2=\frac{D^2}{L_1^2}\{\exp[-\Psi(\zeta)]+\Psi(\zeta)+c\}$$

or

$$\frac{d\Psi(\zeta)}{d\zeta}=\mp a\sqrt{\exp[-\Psi(\zeta)]+\Psi(\zeta)+c}, \tag{12}$$

where the negative sign is associated with anodic polarization $(\Psi_0>0)$ and the positive sign with cathodic polarization $(\Psi_0<0)$. Also,

$$a=\frac{D}{L_1} \tag{13}$$

and the integration constant c should be greater than -1.

Let us now use the condition (11)

$$\frac{1}{\delta}\int_0^{\delta}\exp[-\Psi(\zeta)]d\zeta=-\frac{2}{a^2\delta}\int_0^{\delta}\frac{d^2\Psi(\zeta)}{d\zeta^2}d\zeta+1=1, \tag{14}$$

that is,

$$\int_0^{\delta}d\left(\frac{d\Psi(\zeta)}{d\zeta}\right)=0\Rightarrow\left.\frac{d\Psi(\zeta)}{d\zeta}\right|_0=\left.\frac{d\Psi(\zeta)}{d\zeta}\right|_{\delta}. \tag{15}$$

Using now Eq. (12) one gets

$$\exp[-\Psi(\delta)]+\Psi(\delta)=\exp[-\Psi(0)]+\Psi(0). \tag{16}$$

Remembering expressions (4), one has

$$\Psi_1(0)=\Psi_0=\Psi_1(\bar{\zeta})+\Psi(0)\quad\text{and}$$

$$\Psi_1(\delta)=\Psi_1(\bar{\zeta})+\Psi(\delta)=\Psi_0+\Psi(\delta)-\Psi(0)$$

or

$$\Psi(\delta)=\Psi_1(\delta)-\Psi_0+\Psi(0). \tag{17}$$

Equation (16) becomes

$$\exp[\Psi_0-\Psi_1(\delta)]\exp[-\Psi(0)]+[\Psi_1(\delta)-\Psi_0]+\Psi(0)=\exp[-\Psi(0)]+\Psi(0)$$

or

$$\Psi_1(\delta)-\Psi_0=e^{-\Psi(0)}[1-e^{[\Psi_0-\Psi_1(\delta)]}],$$

i.e.,

$$\Psi(0)=\ln\left[\frac{e^{[\Psi_0-\Psi_1(\delta)]}-1}{\Psi_0-\Psi_1(\delta)}\right]. \tag{18}$$

Let us now integrate Eq. (12),

$$\int_{\Psi(0)}^{\Psi(\zeta)}\frac{d\phi}{\sqrt{\exp(-\phi)+\phi+c}}=\mp a\int_0^{\zeta}d\zeta=\mp a\zeta. \tag{19}$$

For $\zeta=\delta$ the previous expression becomes

$$\int_{\Psi(0)}^{\Psi(\delta)}\frac{d\phi}{\sqrt{\exp(-\phi)+\phi+c}}=\mp a\delta. \tag{20}$$

Using Eqs. (17) and (18), $\Psi(\delta)$ may be expressed in terms of $\Psi_1(\delta)$—the potential on the WO_3–liquid-crystal interface—and Ψ_0, which is known,

$$\Psi(\delta)=\Psi_1(\delta)-\Psi_0+\ln\left[\frac{e^{[\Psi_0-\Psi_1(\delta)]}-1}{\Psi_0-\Psi_1(\delta)}\right]. \tag{21}$$

The integral in Eq. (20) depends on the characteristics of the cell (a,δ), the applied voltage Ψ_0, and also on two unknowns $\Psi_1(\delta)$ and c. The integral can be done numerically for a set of values for $\Psi_1(\delta)$ (between 0 and Ψ_0) and for a set of values for c. The minimum value of the potential slope—i.e., $d\Psi/d\zeta$—occurs when $\Psi=\Psi(\bar{\zeta})=0$ and is $a\sqrt{1+c}$. Therefore, $c>-1$. Moreover, the minimum slope cannot be greater than $[\Psi_0-\Psi_1(\delta)]/\delta$, which limits the values of c. Thus, one has to choose the values of c in the set $(-1,-1+[\Psi_0-\Psi_1(\delta)]^2/a^2\delta^2)$. A three-dimensional plot of the numerical values of the integral in Eq. (20) with respect to $\Psi_1(\delta)$ and c represents a surface [let it be $\Sigma(\Psi_1(\delta),c)$]. Intersecting it with the plane $\Sigma=a\delta$, one obtains a curve that gives a connection between c and $\Psi_1(\delta)$, namely, $c=c(\Psi_1(\delta))$. In that manner, the constant c is eliminated and only one parameter $\Psi_1(\delta)$ is left unknown. But, at the WO_3/LC interface, disregarding any trapped charge, one can use the continuity relations

$$\Psi_1(\delta)=\Psi_2(\delta)$$

and

$$\epsilon_1 \left.\frac{d\Psi_1(\zeta)}{d\zeta}\right|_\delta = \epsilon_2 \left.\frac{d\Psi_2(\zeta)}{d\zeta}\right|_\delta \tag{22}$$

connecting the potential $\Psi_1(\zeta)$ defined for $\zeta \in [0,\delta]$ to the potential $\Psi_2(\zeta)$ defined for $\zeta \in [\delta,1]$, i.e., in the liquid crystal region.

Coming back to the expression (19) the integral in the left hand side can also be done numerically for a set of values Ψ [limited by $\Psi(0)$ and $\Psi(\delta)$]. Representing now the set Ψ on the ordinate and the corresponding values of ζ on the abscissa we get the graph of the function $\Psi(\zeta)$. Of course, this procedure can be repeated for several values of $\Psi_1(\delta)$ and one obtains a family of curves $\Psi(\zeta)$ from which one gets the family

$$\Psi_1(\zeta) = \Psi(\zeta) + \Psi_0 - \ln\left[\frac{e^{[\Psi_0 - \Psi_1(\delta)]} - 1}{\Psi_0 - \Psi_1(\delta)}\right]. \tag{23}$$

We can now consider that in the liquid crystal there are positive and negative ions free to move, either as ionic impurities or as the equilibrium dissociation of liquid crystal molecules themselves [11].

Let $n_p(\zeta)$ and $n_n(\zeta)$ be the concentrations of positive and negative ions, respectively. At equilibrium or very close to equilibrium (as the power dissipated in the sample is quite small $\sim 0.1\ \mu\mathrm{W/cm^2}$) the values of the concentrations are

$$n_p(\zeta) = n_p(\overline{\zeta})\exp[-\Psi_2(\zeta) + \Psi_2(\overline{\zeta})],$$

$$n_n(\zeta) = n_n(\overline{\zeta})\exp[\Psi_2(\zeta) - \Psi_2(\overline{\zeta})], \tag{24}$$

where

$$\Psi_2(\zeta) = \frac{eV(\zeta)}{kT} \quad \text{for} \quad \delta \leqslant \zeta \leqslant 1 \quad \text{and} \quad \Psi_2(1) = 0, \tag{25}$$

that is, $\Psi_2(\zeta)$ is the adimensional potential within the liquid crystal region.

It is easy to verify that the product of the concentrations does not depend on ζ and may be called n_i^2 (a constant),

$$n_p(\zeta)n_n(\zeta) = n_p(\overline{\zeta})n_n(\overline{\zeta}) = n_i^2. \tag{26}$$

One may recognize a well known formula in the physics of semiconductors. The values $\overline{\zeta}$ can conveniently be chosen as that value of ζ for which the two concentrations are equal, i.e.,

$$n_p(\overline{\zeta}) = n_n(\overline{\zeta}) = n_i. \tag{27}$$

In the liquid crystal zone $\delta \leqslant \zeta \leqslant 1$, where ϵ_2 is the dielectric constant of the liquid crystal, the Poisson equation is now

$$\begin{aligned}\frac{d^2\Psi_2(\zeta)}{d\zeta^2} &= -\frac{e^2D^2}{\epsilon_2\epsilon_0 kT}[n_p(\zeta) - n_n(\zeta)]\\ &= -\frac{e^2 n_i D^2}{\epsilon_2\epsilon_0 kT}\{\exp[-\Psi_2(\zeta) + \Psi_2(\overline{\zeta})]\\ &\quad - \exp[\Psi_2(\zeta) - \Psi_2(\overline{\zeta})]\}.\end{aligned} \tag{28}$$

Then,

$$\frac{d^2\Psi_2(\zeta)}{d\zeta^2} = \frac{D^2}{L_2^2}\sinh[\Psi_2(\zeta) - \Psi_2(\overline{\zeta})], \tag{29}$$

where

$$L_2^2 = \frac{\epsilon_2\epsilon_0 kT}{2e^2 n_i}. \tag{30}$$

L_2 plays the role of the Debye length for the liquid crystal zone.

Due to the symmetry of the problem in the liquid crystal region, $\overline{\zeta}$ would be the middle point, i.e., $\overline{\zeta} = (1+\delta)/2$ and $\Psi_2(\overline{\zeta}) = \frac{1}{2}\Psi_1(\delta)$. A rigorous proof of this assertion is given in the Appendix.

To simplify the notation, we set

$$\varphi(\zeta) = \Psi_2(\zeta) - \Psi_2(\overline{\zeta}). \tag{31}$$

$\Psi_2(\overline{\zeta})$ and Ψ_0 being constants, we have

$$\frac{d\Psi_2(\zeta)}{d\zeta} = \frac{d\varphi(\zeta)}{d\zeta}, \quad \frac{d^2\Psi_2(\zeta)}{d^2\zeta} = \frac{d^2\varphi(\zeta)}{d^2\zeta}, \tag{32}$$

as well as the useful expressions

$$\Psi_2(\zeta) = \varphi(\zeta) + \Psi_2(\overline{\zeta}),$$

$$\varphi(1) = -\Psi_2(\overline{\zeta}) = -\tfrac{1}{2}\Psi_1(\delta), \quad \varphi(\delta) = \tfrac{1}{2}\Psi_1(\delta). \tag{33}$$

It can be seen that the equation

$$\frac{d^2\varphi(\zeta)}{d\zeta^2} = \frac{D^2}{L_2^2}\sinh[\varphi(\zeta)] \tag{34}$$

is equivalent to

$$\left(\frac{d\varphi(\zeta)}{d\zeta}\right)^2 = \frac{2D^2}{L_2^2}\cosh[\varphi(\zeta)] + c', \tag{35}$$

where c' is another integration constant to be determined. To do this we may use the fact that

$$\epsilon_2 \left.\frac{d\Psi_2(\zeta)}{d\zeta}\right|_\delta = \epsilon_1 \left.\frac{d\Psi_1(\zeta)}{d\zeta}\right|_\delta \tag{36}$$

and

$$\left(\frac{\epsilon_1}{\epsilon_2}\right)^2\left(\frac{d\Psi_1(\zeta)}{d\zeta}\right)^2_\delta=\left(\frac{d\Psi_2(\zeta)}{d\zeta}\right)^2_\delta=\frac{2D^2}{L_2^2}\cosh[\varphi(\delta)]+c'. \tag{37}$$

So the constant c' is determined and one has

$$\left(\frac{d\Psi_2(\zeta)}{d\zeta}\right)^2=\frac{2D^2}{L_2^2}\left[\cosh[\varphi(\zeta)]-\cosh[\tfrac{1}{2}\Psi_1(\delta)]+\frac{L_2^2}{2D^2}\left(\frac{\epsilon_1}{\epsilon_2}\right)^2\left(\frac{d\Psi_1(\zeta)}{d\zeta}\right)^2_\delta\right]$$
$$=\frac{2D^2}{L_2^2}\{\cosh[\varphi(\zeta)]+u\}=b^2\{\cosh[\varphi(\zeta)]+u\}, \tag{38}$$

where $b^2=2D^2/L_2^2$. The remainder u depends (apart from the parameters of the cell) only on $\Psi_1(\delta)$.

Now we can write

$$\frac{d\varphi(\zeta)}{d\zeta}=\mp b\sqrt{\cosh[\varphi(\zeta)]+u}, \tag{39}$$

where the upper sign corresponds to anodic polarization and the lower sign to cathodic polarization. Let us integrate the previous relation

$$\int_{\varphi(\delta)}^{\varphi(\zeta)}\frac{d\phi}{\sqrt{\cosh\phi+u}}=\mp b\int_\delta^\zeta d\zeta=\mp b(\zeta-\delta)$$
$$=-\frac{2i[F(i\varphi(\zeta)/2|2/(1+u))-F(i\varphi(\delta)/2|2/(1+u))]}{\sqrt{1+u}}, \tag{40}$$

where $F(\varphi|k)=\int_0^\varphi d\phi/\sqrt{1-k\sin^2\phi}$ is the elliptic integral of the first kind.

Letting ζ be equal to 1, we have

$$\int_{\varphi(\delta)}^{\varphi(1)}\frac{d\phi}{\sqrt{\cosh\phi+u}}=\int_{\Psi_1(\delta)/2}^{-\Psi_1(\delta)/2}\frac{d\phi}{\sqrt{\cosh\phi+u}}=\mp b(1-\delta). \tag{41}$$

The left hand side depends on the parameter $\Psi_1(\delta)$ which now can be determined numerically. Then, coming back to the expression (40) we can calculate the right hand side of it for a sufficient number of values φ. We obtain the function $\zeta(\varphi)$ numerically and by reversing the plot this gives us $\varphi(\zeta)$, and therefore $\Psi_2(\zeta)$. This function can be plotted for both anodic and cathodic polarizations. Knowing that $E_2(\zeta)=-(kT/eD)[d\Psi_2(\zeta)/d\zeta]$ is the electric field inside the liquid crystal and that $-\epsilon_2\epsilon_0(kT/eD^2)[d^2\Psi_2(\zeta)/d\zeta^2]$ gives us the total charge density as a function of $\zeta\in[\delta,1]$ one can plot the electric potential, the electric field, and the electric charge.

TABLE I. Estimated values for the parameters used in the calculations. WO$_3$ parameters for the anodic and cathodic polarization: stored charge density, n, the concentration of negative charges OH$^-$; L_1, the Debye screening length. Liquid crystal (E7) parameters: n_i, the ion concentration in the liquid crystal; L_2, the Debye screening length in a liquid crystal.

WO$_3$, $\epsilon_1\approx6$, $d=0.4\ \mu$m, $\delta=0.05$, $S=2$ cm^2		
	Anodic (3 V)	Cathodic (−3 V)
Charge (μC/cm^2)	0.36	0.12
n (10^{21} m^{-3})	60	20
L_1 (nm)	10	17
a	800	450
$a\delta$	40	22
Liquid crystal (E7), $\epsilon_2\approx10$, $D=8\ \mu$m		
n_i (10^{18} m^{-3})		6
L_2 (μm)		1
b		11.6
$b(1-\delta)$		11

The experimental results presented above indicated a stored charge density of around 0.36 μC/cm^2 in the anodic case (+3 V) and 0.12 μC/cm^2 in the cathodic case (−3 V). In the two cases, from these values, we can estimate the concentration n of negative charges OH$^-$ in the WO$_3$ film: 60×10^{21} and 20×10^{21} m^{-3}. As far as the parameters of the liquid crystal are concerned, the concentration of charges should not depend on the polarization of the cell, the injection of charges being small. A typical value of L_2 of $\approx1\ \mu$m is reported in the literature [11,12]. It corresponds to an intrinsic concentration n_i of the order of 6×10^{18} m^{-3}. This concentration can be obtained assuming only a dissociation rate of 10^{-9}, to say nothing of the ionic impurities. In Table 1 we present the estimated values for the parameters used in the calculations.

$$\text{WO}_3,\ \epsilon_1\approx6,\ d=0.4\ \mu\text{m},\quad \delta=0.05,\quad S=2\ \text{cm}^2.$$

With the values mentioned in Table I one may see that in order to have the value of the integral in Eq. (20) equal to $a\delta=40$ one must consider $c\simeq-1$ for any value of $\Psi_1(\delta)$ in the physical range. A further simplification appears if we consider the value of $\Psi_0-\Psi_1(\delta)$ which is the (adimensional) voltage drop across the WO$_3$ film. If $\Psi_0\approx115$, i.e., $V(0)=3$ V, then, even if $\Psi_0-\Psi_1(\delta)$ is only 10% of $\Psi_0, e^{\Psi_0-\Psi_1(\delta)}\gg1$, so we can use the approximate expressions

$$\Psi(\delta)\approx-\ln[\Psi_0-\Psi_1(\delta)],$$
$$\Psi(0)\approx\Psi_0-\Psi_1(\delta)-\ln[\Psi_0-\Psi_1(\delta)], \tag{42}$$

which simplifies the computations. With the above mentioned considerations one can determine the value of $\Psi_1(\delta)$ by means of Eq. (41) and then $\Psi_1(\zeta)$ and $\Psi_2(\zeta)$. In practice, due to the fact that $c\approx-1$ it is not easy to find the function $c=c(\Psi_1(\delta))$ as discussed earlier. In fact, it is more convenient to perform a small number of iterations until Eqs.

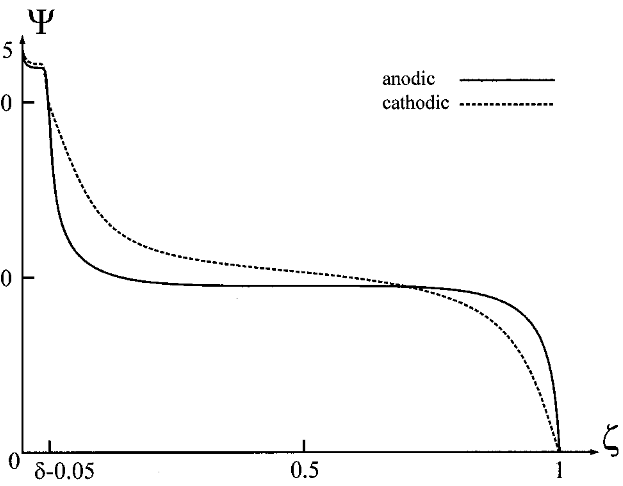

FIG. 10. A plot of numerical calculations of the potential for both WO_3 and liquid crystal regions. Absolute values were used in both cases.

(41) and (20) are fully satisfied with the same value of $\Psi_1(\delta)$. The numerical calculations for $\Psi_1(\zeta)$ and $\Psi_2(\zeta)$ are plotted in Fig. 10. The result is consistent with the general trend that was anticipated qualitatively in Fig. 9.

IV. CONCLUSIONS

In this paper we have presented experimental facts that suggest an explanation of the asymmetric electro-optical behavior of a NLC cell with an inserted layer of WO_3. The idea of an internal counterfield, which lowers the total electric field in the bulk of the LC below the transition threshold, has already been discussed in Ref. [4]. In the same paper, a method of measuring the intensity of this field was presented. Now, we go a step forward by making a direct connection between this counterfield and the electrochemical processes inside the layer of WO_3. We consider that the most important fact is the asymmetric creation or annihilation of positive charges (protons) in the tungsten trioxide layer together with the fact that the positive charges are mobile whereas the negative charges (OH^-) are essentially fixed. The experiments have shown that in the case of anodic polarization the total charge stored in the cell is approximately three times higher than in the case of cathodic polarization. Yet this single fact might not explain the asymmetric behavior of the cell. We also have to consider the mobility of the positive charges in WO_3.

First, let us analyze the case of anodic polarization. Protons are pushed toward the right ($\zeta=\delta$), leaving on the ITO-WO_3 interface a layer (about $L_1 \approx 10$ nm thick) of essentially pure negative charge which attracts an equal positive charge on the ITO side. As a consequence, an equivalent negative charge appears on the other ITO side ($\zeta=1$). This, in turn, mobilizes the positive ions of the liquid crystal and so the counterfield sets in.

In the case of cathodic polarization, apart from the fact that the positive charge in WO_3 is now smaller, the ITO-WO_3 interface attracts protons. The buildup of surface charge will be smaller because the negative ions (OH^-) are not mobile. A smaller amount of negative charge in the ITO region is now attracted and the surface charges in the NLC are now much smaller, thus decreasing the counterfield.

In fact, in both cases, the fields near the interfaces are given by $\sigma/2\epsilon\epsilon_0$. With the anodic polarization, from the arguments presented before, one may consider that σ is essentially the total measured charge q divided by the area of the interface. On the contrary, in the cathodic case, the measured charge $q' \approx \frac{1}{3}q$ is no longer concentrated only on the surface, so $\sigma' < \frac{1}{3}\sigma$.

A theoretical model combining statistical physics with pertinent electrostatic equations was developed, and this theory can be applied or extended to any other similar system. As a matter of fact we have used these ideas when replacing the WO_3 layer (which is difficult to obtain) with a layer of polymers doped with free protons [5].

ACKNOWLEDGMENTS

A.L. A.-I., and A.Th.I. have the pleasure of noting the hospitality of the Calabrian Liquid Crystal Group. This work was partially supported by Inco Copernicus Program No. IC15-CT98-0806, and was carried out in the framework of the Italian MURST research project ''Piani di Potenziamento della Rete Scientifica e Tecnologica,'' Cluster No. 26-P4W3.

APPENDIX

Considering that the liquid crystal zone is electrically neutral, one has

$$\int_{\delta}^{1}[n_p(\zeta)-n_n(\zeta)]d\zeta=0 \tag{A1}$$

or, taking into account Eq. (28),

$$\int_{\delta}^{1}\frac{d^2\Psi_2(\zeta)}{d\zeta^2}d\zeta=\left.\frac{d\Psi_2(\zeta)}{d\zeta}\right|_1-\left.\frac{d\Psi_2(\zeta)}{d\zeta}\right|_\delta=0,$$

that is,

$$\left.\frac{d\Psi_2(\zeta)}{d\zeta}\right|_\delta=\left.\frac{d\Psi_2(\zeta)}{d\zeta}\right|_1. \tag{A2}$$

The same relation being true for $\varphi(\zeta)$, one has the equation

$$\mp b\sqrt{\cosh[\varphi(\delta)]+u}=\mp b\sqrt{\cosh[\varphi(\delta)]+u} \tag{A3}$$

or

$$\cosh[\varphi(\delta)]=\cosh[\varphi(1)] \tag{A4}$$

with two solutions: either $\varphi(\delta)=\varphi(1)$, which must be rejected because it describes a short-circuit case, or $\varphi(\delta)=-\varphi(1)$. Then

$$\Psi_2(\delta)-\Psi_2(\overline{\zeta})=\Psi_2(\overline{\zeta})-\Psi_2(1),$$

but $\Psi_2(1)=0$, and one gets

$$\Psi_2(\overline{\zeta})=\tfrac{1}{2}\Psi_2(\delta)=\tfrac{1}{2}\Psi_1(\delta). \quad \text{Q.E.D.} \tag{A5}$$

[1] R. Bartolino, N. Scaramuzza, D. E. Lucchetta, E. S. Barna, A. Th. Ionescu, and L. M. Blinov, J. Appl. Phys. **85**, 2870 (1999).
[2] G. Strangi, D. E. Lucchetta, E. Cazzanelli, N. Scaramuzza, and C. Versace, Appl. Phys. Lett. **74**, 534 (1999).
[3] E. Cazzanelli, N. Scaramuzza, G. Strangi, C. Versace, A. Pennisi, and F. Simone, Electrochim. Acta **44**, 3101 (1999).
[4] G. Strangi, E. Cazzanelli, N. Scaramuzza, C. Versace, and R. Bartolino, Phys. Rev. E **62**, 2263 (2000).
[5] A.-L. Alexe-Ionescu *et al.* (unpublished).
[6] C. G. Granqvist, Appl. Phys. A: Solids Surf. **57**, 3 (1993).
[7] C. G. Granqvist, Solid State Ionics **53–56**, 479 (1992).
[8] J. Vondrak and J. Bludska, Solid State Ionics **68**, 317 (1994).
[9] Reactions can be more complicated, for example, some of the H^+ can attach to water molecules giving hydronium ions $(H_3O)^+$ with lower mobility than that of protons.
[10] D. Dini, F. Decker, and E. Masetti, J. Appl. Electrochem. **26**, 647 (1996).
[11] G. Barbero, A. K. Zvezdin, and L. R. Evangelista, Phys. Rev. E **59**, 1846 (1999).
[12] R. N. Thurston, J. Cheng, R. B. Meyer, and G. D. Boyd, J. Appl. Phys. **56**, 264 (1984).